

Human Powered Hydrofoil Design & Analytic Wing Optimization

Andy Gunkler and Dr. C. Mark Archibald
Grove City College
Grove City, PA 16127
Email: gunklerwal@gcc.edu

Abstract –

Human powered hydrofoil watercraft can have marked performance advantages over displacement-hull craft, but pose significant engineering challenges. The focus of this hydrofoil independent research project was two-fold. First of all, a general vehicle configuration was developed. Secondly, a thorough optimization process was developed for designing lifting foils that are highly efficient over a wide range of speeds. Given a well-defined set of design specifications, such as vehicle weight and desired top speed, an optimal horizontal, non-surface-piercing wing can be engineered. Design variables include foil span, area, planform shape, and airfoil cross section. The optimization begins with analytical expressions of hydrodynamic characteristics such as lift, profile drag, induced drag, surface wave drag, and interference drag. Research of optimization processes developed in the past illuminated instances in which coefficients of lift and drag were assumed to be constant. These shortcuts, made presumably for the sake of simplicity, lead to grossly erroneous regions of calculated drag. The optimization process developed for this study more accurately computes profile drag forces by making use of a variable coefficient of drag which, was found to be a function of the characteristic Reynolds number, required coefficient of lift, and airfoil section. At the desired cruising speed, total drag is minimized while lift is maximized. Next, a strength and rigidity analysis of the foil eliminates designs for which the hydrodynamic parameters produce structurally unsound wings. Incorporating constraints on minimum takeoff speed and power required to stay foil-borne isolates a set of optimized design parameters. This method was used to engineer a foil for a medium-distance, high-performance human-powered watercraft. This foil should be able to takeoff at moderate speeds and remains flying with minimal power for extended duration, while exhibiting suitable stability and maneuverability characteristics.

All hydrodynamic and structural characteristics such as lift, drag, Reynolds number, wing loading and airfoil cross sectional area moment of inertia are computed analytically. Compared to testing hours of testing a discrete array of designs using Computational Fluid Dynamics and Finite Element Analysis, this process, finds a truly optimum design for any set of parameters by running a single MATLAB program. Fabrication and testing of this foil will be completed in the future in conjunction with building a viable, operational vehicle.

Introduction and Project Design Specification –

Motivated by general mechanical engineering departmental interest at Grove City College in the science of human powered vehicles, a hydrofoil HPV was designed as part of an independent research project. The project objective was to engineer and build a human powered hydrofoil boat capable of traveling 2000 meters in less than 6 minutes and 46 seconds.¹ By beating this time, which is the current Jr. Men's Single Scull rowing world record, hydrofoil performance will be proven to be superior to the best displacement hull vehicles. Whereas rowing at such speeds can only be attained by world class athletes, foiling at an average speed of 4.9 m/s (vehicle design speed) is expected to be attainable by a man of average fitness and build. Additionally, to ensure vehicle versatility, top speed must exceed 7 m/s yet takeoff must occur at speeds below 3.6 m/s.

Vehicle Design Rationale –

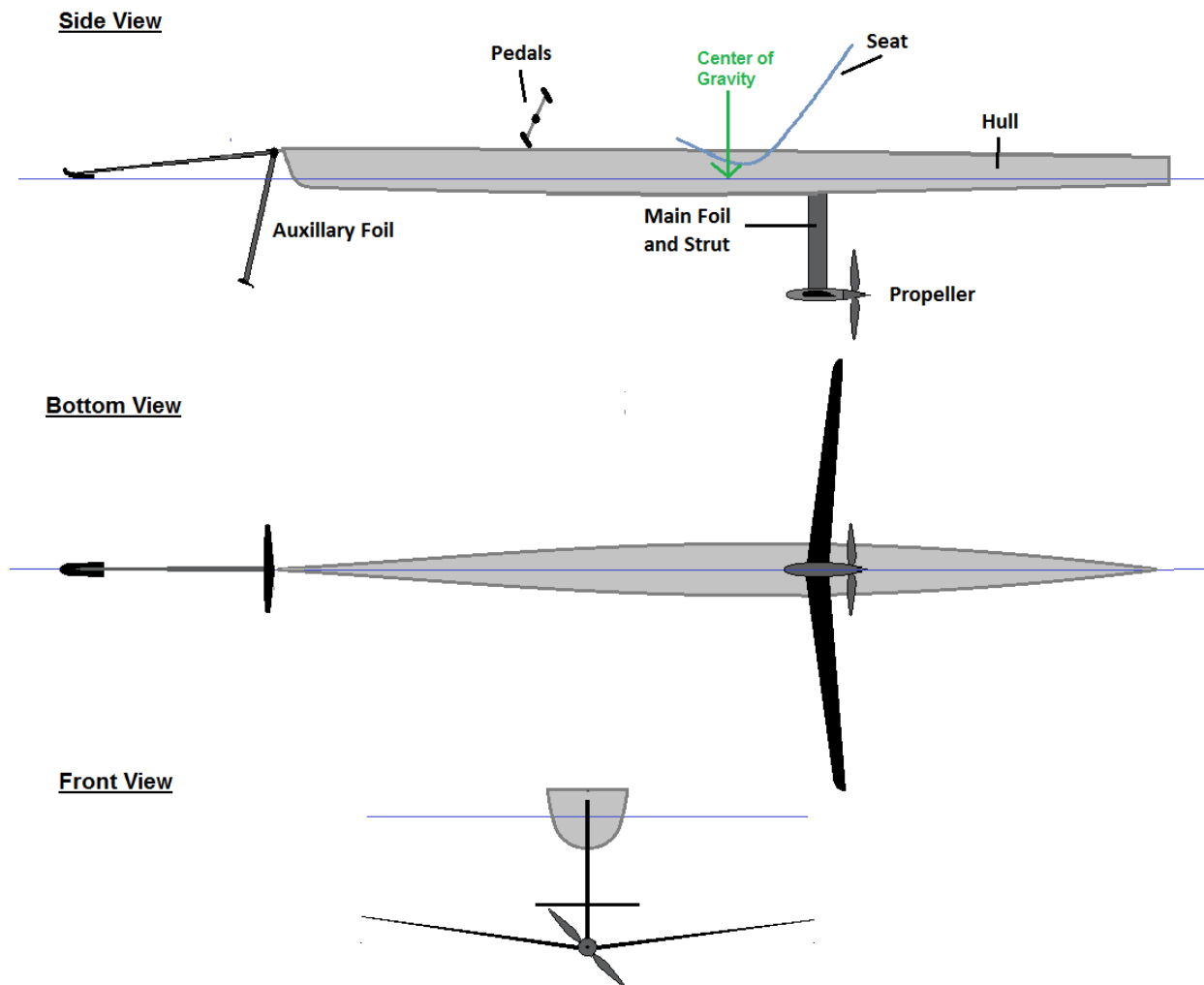


Figure 1. Vehicle Configuration Schematic

The fundamental defining aspect of the hydrofoil platform shown in Figure 1 is the use of T-foils. There are two main categories of hydrofoils: T-foils, which look like inverted T's and V-foils, which resemble the letter V. V-foils have been successfully implemented on many powerboats and initially seem like a suitable candidate for human powered vehicles as well. However, their design is inherently inefficient.

At low speeds, the majority of the V-foil is submerged and substantial lift is produced. As speed increases, the lift per unit area increases so the vehicle begins to rise out of the water. As portions of the foil lift free from the water, drag decreases which allows for a further increase in speed². This design inherently maintains stable equilibrium between lift and weight. V-foils are also self leveling. As the vehicle rolls to one side, more of the lifting surface is submerged and the foil on the opposite side is lifted out of the water. The resultant asymmetrical lift counteracts the rolling motion and returns the vehicle to level flight.

The positive traits outlined above are overshadowed by reduced efficiency. The geometry of the foil platform amplifies profile drag and drag due to lift. As a result of the two halves of the foil being oriented at an angle, two opposing horizontal components of force are also produced. The by-product of lift produced by a foil is drag. Therefore, for angled foils, the unnecessary lift results in unnecessary drag. Profile drag, also known as form drag, arises from the forces and energy losses associated with the direction change of a fluid as it flows around an object. The profile drag of a specific foil section is a function of Reynolds Number and foil size. Compared to a horizontal T-foil of the same foil cross-section operating at the same speed, and hence the same Reynolds number, the only difference between hydrofoil configurations is the difference between the foils' spans. Therefore, the difference in profile drag is proportional to these differing lengths.

The most pronounced factor that decreases the efficiency of V-foils is the ventilation of the surface-piercing foils. All subcavitating foils create lift by developing a low pressure region on the upper camber (surface) and a high pressure on the lower camber. If the low pressure drops substantially, the resulting pressure differential between this vacuum and the atmosphere can introduce air along the leading edge³. This turbulent mixture between water and air can significantly increase drag and possibly stall major portions of the foil. The following account of early versions of MIT's "Decavitator" HPV hydrofoil substantiates the theoretically flawed nature of V-foils.

"The V-foil design included twin wooden hulls, a 10ft diameter air propellor, a triangular fuselage based loosely on the Daedalus layout, and a surface-piercing V-foil with a 10ft span. Primary test pilot Mark Drela and heavyweight test pilot Matthew Wall quickly discovered the ventilation problems inherent to the V-foil design. This version of the boat was not stable in pitch, nor was the pilot able to bring the boat onto the foils under his own power. Tow tests revealed serious ventilation problems with the V-foil design..."⁴

T- Foils are very efficient compared to V-foils for three reasons. First of all, all lift is vertical so there is no drag due superfluous horizontal components of lift. Secondly, the planform shape of the T-foil can be optimized so as to minimize induced drag. Finally, ventilation is not a significant issue.

The lifting foil is not surface-piercing and the vertical strut, although surface-piercing, does not need to create lift. Therefore, the strut foil section can be such that no sharp low pressure regions form along the foil. As a result, there is less of a tendency for air to be introduced along the span of the strut.

In light of their obvious hydrodynamic superiority, T-foils present unique design challenges. First of all, unlike V-foils, T foils do not automatically balance lift with the weight of the vehicle. Instead, the lift produced by the fully submerged foil is proportional to speed. Therefore, a T-foil that is capable of a relatively low-speed takeoff will produce excess lift at higher speeds. The imbalance of vertical forces due to the extra lift causes the vehicle to rise continuously. Upon reaching the surface, the hydrofoil is subject to two drag-inducing effects. Sudden and complete ventilation can stall the foil, eradicate lift, and cause the vehicle to crash violently back into the water. Even if catastrophic ventilation does not occur, operating close to the surface leads to an increase in induced drag.

Allan Abbott, author of *Human Powered Vehicles* and the designer of the record breaking “Flying Fish II” hydrofoil, explains that when the depth of the foil below the surface of the water is less than one chord-length, induced drag is doubled.⁵

Due to the possibility of complete ventilation as well as significantly increased drag, the lift created by the hydrofoil must be controlled so that the lifting foil flies steadily at the optimum height.

The automatic height control uses a water surface following device to sense flying height and a mechanism for varying lift. Just as an airplane uses flaps on takeoff to increase lift at low speeds, so too could a HPV hydrofoil. A flap system increases the camber of a foil which increases lift at the penalty of increased drag. Existing hydrofoils have implemented a single, plain flap connected to the main foil using a flexible membrane. While capable of creating the high coefficient of lift required for flight at low speeds, the large gap in the lower camber during cruising configuration would be an unacceptable source of drag. A foil with variable angle of attack, while potentially requiring more complex mechanical components, could be most efficient over the wide range of required coefficients of lift.

An HPV hydrofoil must be balanced fore and aft just like any other vehicle. Some vehicles such as cars and bicycles are supported evenly with main wheels bearing the same load in the front and in the rear. The logical, but flawed, parallel for a hydrofoil would be two main lifting foils, one in the front and one in the back. First of all, the rear foil would operate in the turbulent wake of the front foil. Secondly, the weight of the rider, which is the most significant load on the vehicle, is bridged between the two lift forces. The additional structure required to support this would add extra weight to the vehicle. A human powered hydrofoil boat is best configured like an airplane with the majority of lift being produced by main wing. The lifting hydrofoil will operate efficiently in undisturbed flow and be positioned nearly directly under the rider. An auxiliary lifting foil mounted near the bow of the boat will provide pitch control. While the details of the required mechanism are beyond the scope of this paper, both lifting hydrofoils will be variable angle of attack to provide variable coefficients of lift.

Roll stability is result of the dihedral effect. Dihedral refers to the upswept angle from the root of the foil to the tip.⁶ The front-view of the vehicle schematic in Figure 1 shows the dihedral angle of the main foil. When a dihedral lifting surface rolls, asymmetric lift causes the vehicle to slip sideways. This side-slip increases the angle of attack of the low wing which increases its lift and levels the vehicle. The sweep angle of the main wing enhances the dihedral effect.⁷

Lifting Foil Optimization –

Upon establishing the general vehicle configuration, an analytic optimization process was developed to identify the best wing design. Since the primary goal is to travel 2000 meters in 6:45, the foils were optimized to be most efficient at this design speed of 4.9 meters per second while being structurally viable and meeting takeoff velocity, sprint speed, and endurance constraints.

The optimization process based upon the general scheme outlined in Allan Abbott’s book “*Human-powered Vehicles*” utilizes four parameters: planform shape, wingspan, aspect ratio, and airfoil cross-section shape.⁸ First of all, an optimum planform shape is chosen. Next the drag force is calculated for every combination of span and aspect ratio. Finally, the span and aspect ratio that produce lowest drag while obeying maximum takeoff velocity and structural constraints are identified. The process is repeated for different applicable stock airfoil cross section until an optimum design is determined.

Planform shape, as shown in the following figure, describes the profile of a lifting foil as seen from above the vehicle, perpendicular to flow.

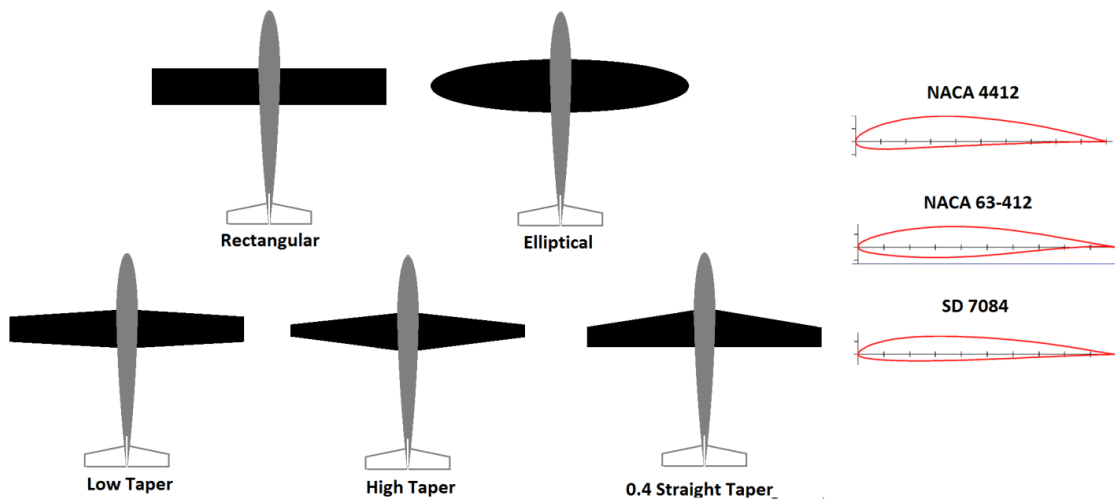


Figure 2. Wing Planform Shapes And Airfoil Section⁹

Wingspan is the distance from tip to tip or the overall width of the foil. Aspect ratio, which is the relative slenderness of a wing planform, is defined by the following formula.¹⁰

$$AR = \frac{Span^2}{Area}$$

Proceedings of the 2011 ASEE NC & IL/IN Section Conference

Copyright © 2011, American Society for Engineering Education

A high aspect ratio yields a slender wing whose chord-length, the distance from a foil's leading edge to trailing edge, is relatively small compared to span. A wing with a low aspect ratio is short and stubby. Planform area is a function of both span and aspect ratio.

To reiterate, the objective was to design a hydrofoil of lowest power consumption which translates to optimum efficiency. Since efficiency is described as the ratio of lift to drag, and lift is held constant so as to balance the weight of the vehicle, drag must be minimized. The two major types of drag are lift-induced drag and profile drag.

Calculation of Drag Forces –

Induced drag is an inherent byproduct of lift that results from energy expended during the equalization of fluid pressure between the two sides of a foil. Sometimes visible on airplanes, trailing vortices form as fluid from the high pressure region beneath the lower camber spills up and around the wingtips. Induced drag is minimized when the fluid pressure differential gradually approaches zero near the tip. An elliptical lift distribution achieves this by causing lift at the tip to approach zero and promoting constant downwash along the trailing edge of the foil.¹¹ Logically, wing loading is roughly proportional to chord-length. Therefore, an elliptic planform shape produces an elliptic distribution of lift which minimizes induced drag. Additionally, according to Abbot, for a "...straight-tapered wing, a taper ratio of 0.4 is about optimum for achieving a nearly elliptical lift distribution."¹² In other words, induced drag is also minimized for a foil whose tip chord-length is 40% of that of the root. Since they are easier to construct yet present no penalty of increased drag, the hydrofoil vehicle designed during this optimization process uses 0.4 tapered straight foils. The following formulas describe induced drag as a function of span.¹³

$$\begin{aligned}
 \text{Induced Drag} &= q \times C_{di} \times \text{Area} & q & \text{Dynamic pressure} \\
 & & C_{di} & \text{Induced Drag Coefficient} \\
 & & \text{Area} & \text{Planform Area} \\
 q &= \frac{1}{2} \times \rho \times V^2 & \rho & \text{Fluid density} \\
 & & V & \text{Flow velocity} \\
 & & f_i & \text{Factor of interference (= 1)} \\
 & & C_l & \text{Coefficient of Lift} \\
 C_{di} &= \frac{f_i \times C_l^2}{\pi \times AR} \\
 C_l &= \frac{w}{q \times \text{Area}} = \frac{w}{\frac{1}{2} \times \rho \times V^2 \times \frac{\text{Span}^2}{AR}} = \frac{2 \times w \times AR}{\rho \times V^2 \times \text{Span}^2} \\
 \text{Induced Drag} &= \frac{\rho \times V^2 \times f_i \times \left(\frac{2 \times w \times AR}{\rho \times V^2 \times \text{span}^2} \right)^2 \times \text{span}^2}{2 \times \pi \times AR^2} = \frac{f_i \times w^2}{\rho \times q \times \text{span}^2}
 \end{aligned}$$

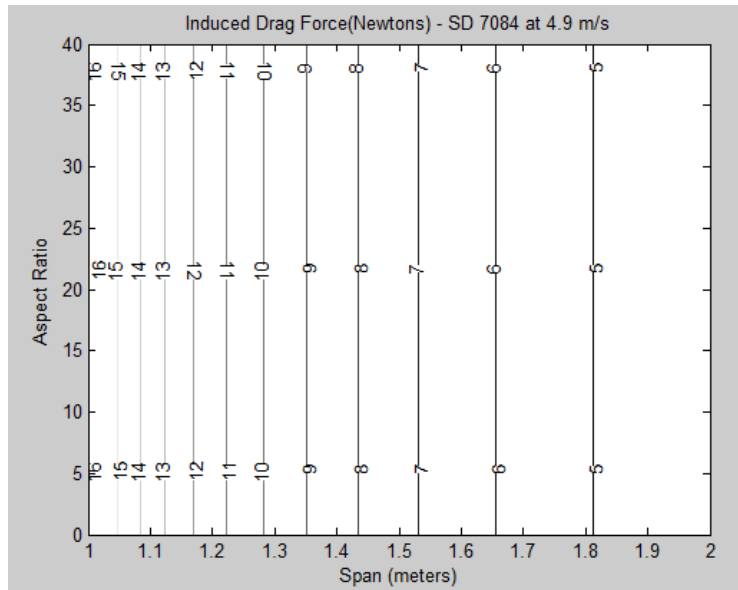


Figure 3. Contour Plot of Induced Drag (for a SD 7084 airfoil). Note, induced-drag is shown to be independent of aspect ratio as wing area varies simultaneously.

Profile drag is the net force required to overcome viscous effects and change the momentum of a fluid as it flows around a solid object. Also known as form drag, forces due to profile drag act in the direction parallel to the flow with a magnitude:

$$ProfileDrag = q \times Area \times Cdp$$

Again, q is simply the dynamic fluid pressure and area is described as the square of span divided by aspect ratio. Instead of assuming a constant coefficient of drag, for the optimization process developed during this research, a variable coefficient of drag was calculated at every combination of span and aspect ratio

Coefficient of drag, in addition to being dependent upon Reynolds Number, is proportional to coefficient of lift because as the angle of attack of a foil increases, lift increases at the penalty of drag.¹⁴ The coefficient of lift required to support the weight of the hydrofoil vehicle and rider is known at all times through the formula:

$$Cl = \frac{w}{q \times Area} = \frac{w}{\frac{1}{2} \times \rho \times V^2 \times \frac{span^2}{AR}} = \frac{2 \times w \times AR}{\rho \times V^2 \times Span^2}$$

Reynolds Number for a wing is related in the following formula¹⁵:

$$RE = \frac{V \times chord \times \rho}{viscosity}$$

Once the required coefficient of lift and operating Reynolds number are known, the coefficient of drag for a certain airfoil section of can be obtained through a graph similar to that shown in Figure 4.

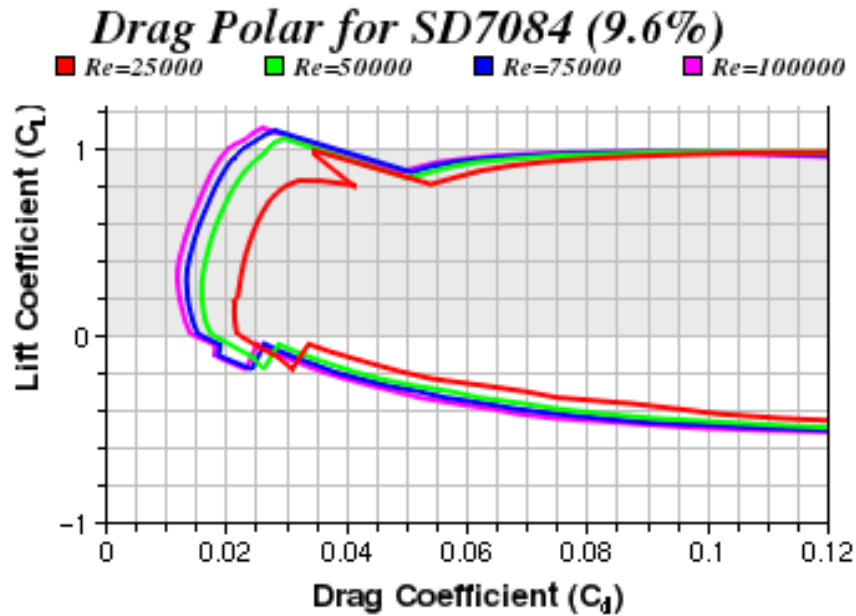


Figure 4. Plot of Coefficient of Lift to Coefficient of Drag at Different Reynolds Numbers¹⁶

A three dimensional surface interpolation of the data from this type of graph was performed so as to analytically relate all possible calculated values of required coefficient of lift at any Reynolds number.

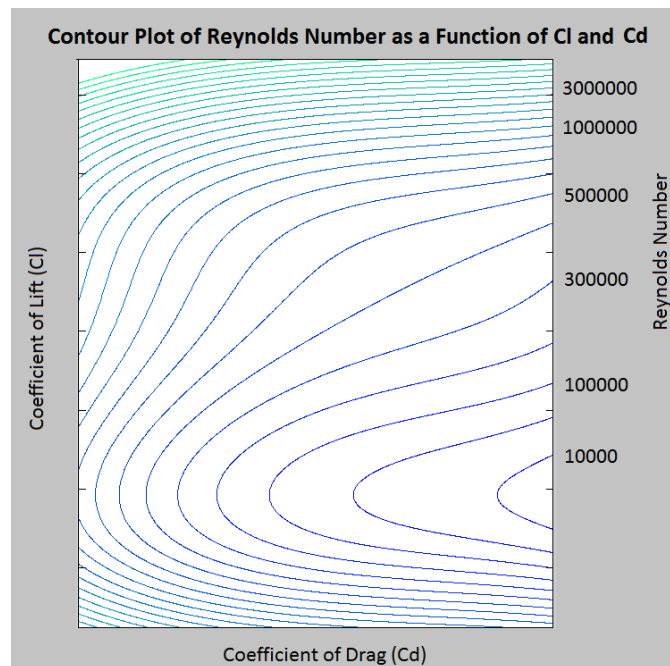


Figure 5 – Contour Plot of the 3-D surface interpolation analytically relating coefficients of lift, coefficient of drag, and Reynolds Number.

Input of Required Coefficient of Lift and Reynolds number into this equation outputs coefficient of drag which allows for a highly accurate calculation of profile drag at each combination of span and aspect ratio.

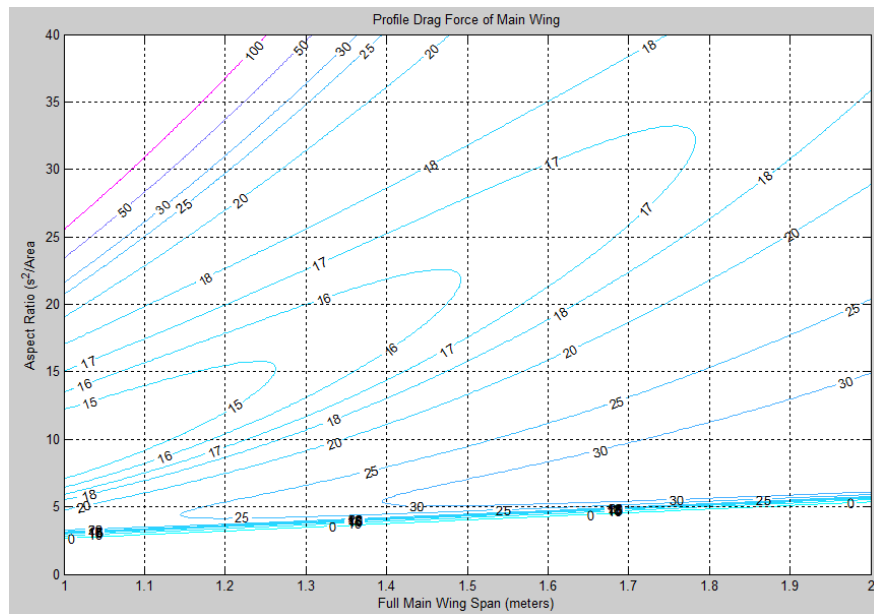


Figure 6. Contour Plot of the Profile Drag Force as a Function of Span and Aspect Ratio.

Total Drag, which is the sum of Induced Drag and Profile Drag, is the synthesis of Figure 3 and Figure 6.

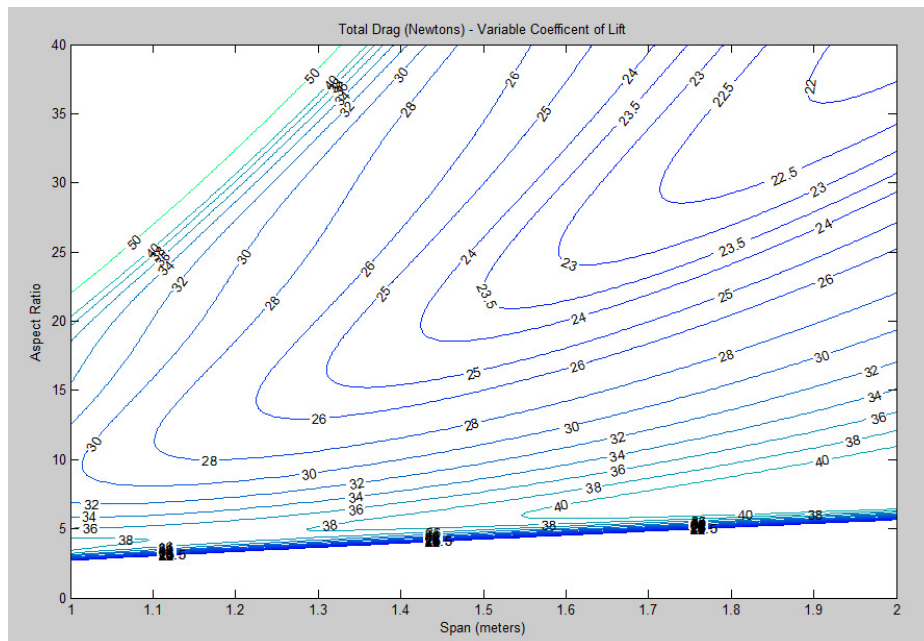


Figure 7 – Contour Plot of the Total Drag Force Developed By the Main Wing

Structural Considerations –

Observation of Figure 7 shows that lowest drag is produced by hydrofoils with large spans and high aspect ratios. However, such wing would be extremely slender and not structurally viable. Therefore, the hydrofoil wings must be constrained by maximum allowable tip deflection and root stress. The maximum allowable height of tip deflection is defined as being five percent of total span. This ensures that lift is predominantly vertical and prevents significant torsional deflection. Any twisting would tend to vary wing angle of attack which would introduce unpredictable hydrodynamic effects. Tip deflections become too large long before root stress becomes significant. Each half of the T-Foil wing is treated as a cantilever beam and a beam analysis was performed to determine which combinations of span and aspect ratio were viable.

The assumed elliptical distribution of lift defines loading as the following function of horizontal distance x along the total span:

$$Loading(x) = \sqrt{\frac{4 \times W^2}{\pi \times span} - \frac{4 \times W^2 \times x^2}{\pi \times span \times \frac{span^2}{2}}}$$

Using the Euler-Bernoulli beam equations, this function was integrated to describe the shear and bending moment functions.¹⁷

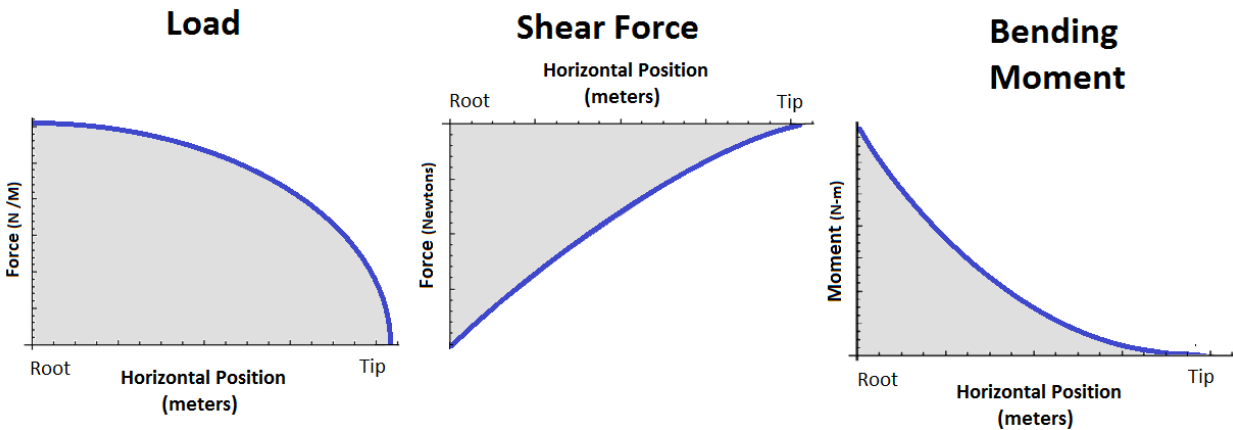


Figure 8 – Load, Shear and Bending Moment Diagrams for an elliptic distribution of lift on a cantilevered wing.

Beam cross sectional moment of inertia and modulus of elasticity must be known in order to calculate the slope of beam deflection. The hydrofoil wings will be solid unidirectional carbon fiber reinforced plastic which has a modulus of elasticity of approximately 135 GPa.¹⁸ The area moment of inertia of each airfoil shape was numerically approximated by dividing the cross-section into numerous trapezoids. Each individual moment of inertia was calculated and then related using the parallel axis theorem to yield the overall area moment of inertia.

The function was integrated numerically to yield the slope of deflection and again to yield tip displacement position. This process is demonstrated graphically in Figure 9.

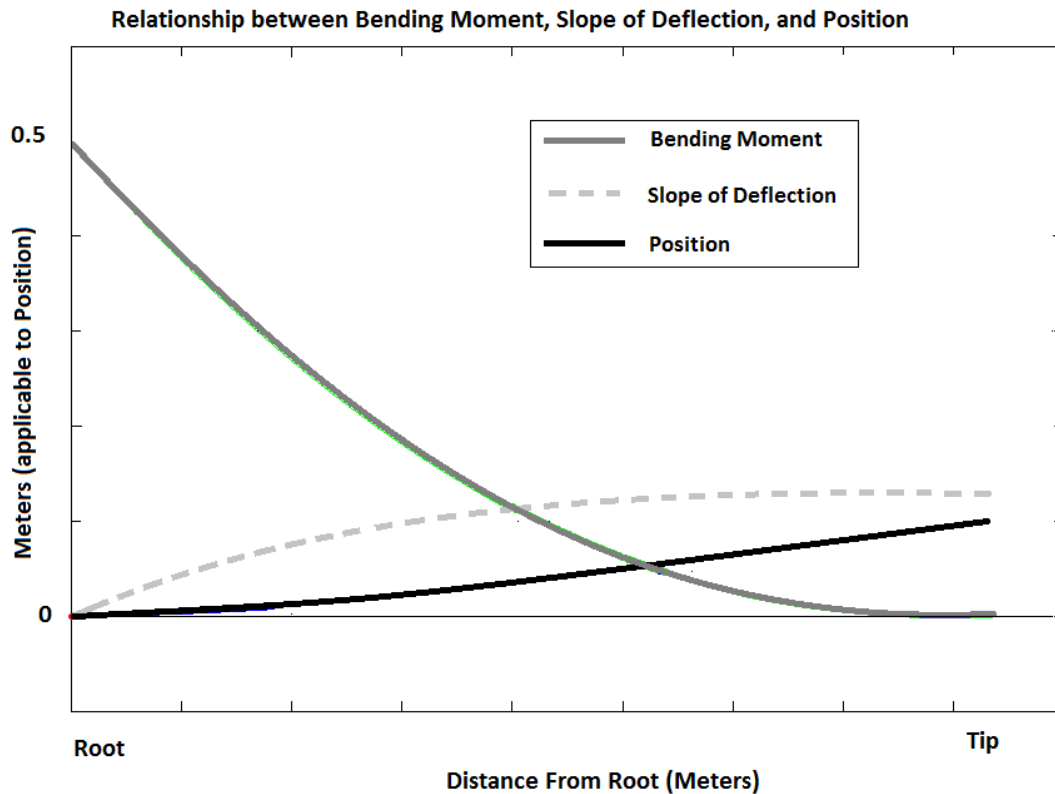


Figure 9 – Plot of the relationship between bending moment, slope of deflection, and position, and normalized tip displacement.

Maximum Takeoff Velocity –

A human powered hydrofoil must accelerate to foiling speed while being supported by displacement hulls. Hull drag is proportional to speed so the vehicle must reach foiling speeds and lift clear of the water before the force of drag exceeds available propulsion power. Velocity at lift off is defined by the following equation¹⁹:

$$Takeoff\ Velocity = \sqrt{\frac{2 \times AR \times W}{\rho \times CL_{max} \times span^2}} \quad (CL_{max} \text{ is the maximum possible coefficient of lift.})$$

Choosing the Optimum Lifting Foil –

Consideration of total drag, structural constraints, and maximum allowable takeoff velocity isolated the optimum parameters for a lifting foil. Additional drag, whether it be from air resistance, the front auxiliary hydrofoil, the vertical struts of the T-foils, or the propeller drive train, was combined added to the drag from the main lifting foil to accurately describe total vehicle drag. Required propulsive power, which is directly proportional to total drag as defined in the following formula, is the fundamental metric used in evaluating hydrofoil design.²⁰

$$\text{Required Power} = \frac{\text{Drag} \times \text{Velocity}}{E} \quad \text{where } E \text{ is total drive-train and propeller efficiency}$$

The lifting foil optimization process was evaluated for NACA 4412 and 63-412 and Selig-Donovan 7084 foil cross sections.

	Power Required at Liftoff Speed (3.5 m/s)	Power Required at Design Velocity (4.9 m/s)	Power Required at High Speed (6.0 m/s)
SD 7084	160 Watts	240 Watts	345 Watts
NACA 63-412	170 Watts	245 Watts	380 Watts
NACA 4412	170 Watts	260 Watts	362 Watts

The SD 7084 foil is most the most efficient foil at cruise and takeoff velocities. All hydrodynamic characteristics, structural calculations, and takeoff constraints were combined into a Matlab program. As the output from this computer program demonstrates, the SD 7084 hydrofoil was found to be the optimum lifting wing for a human powered hydrofoil vehicle.

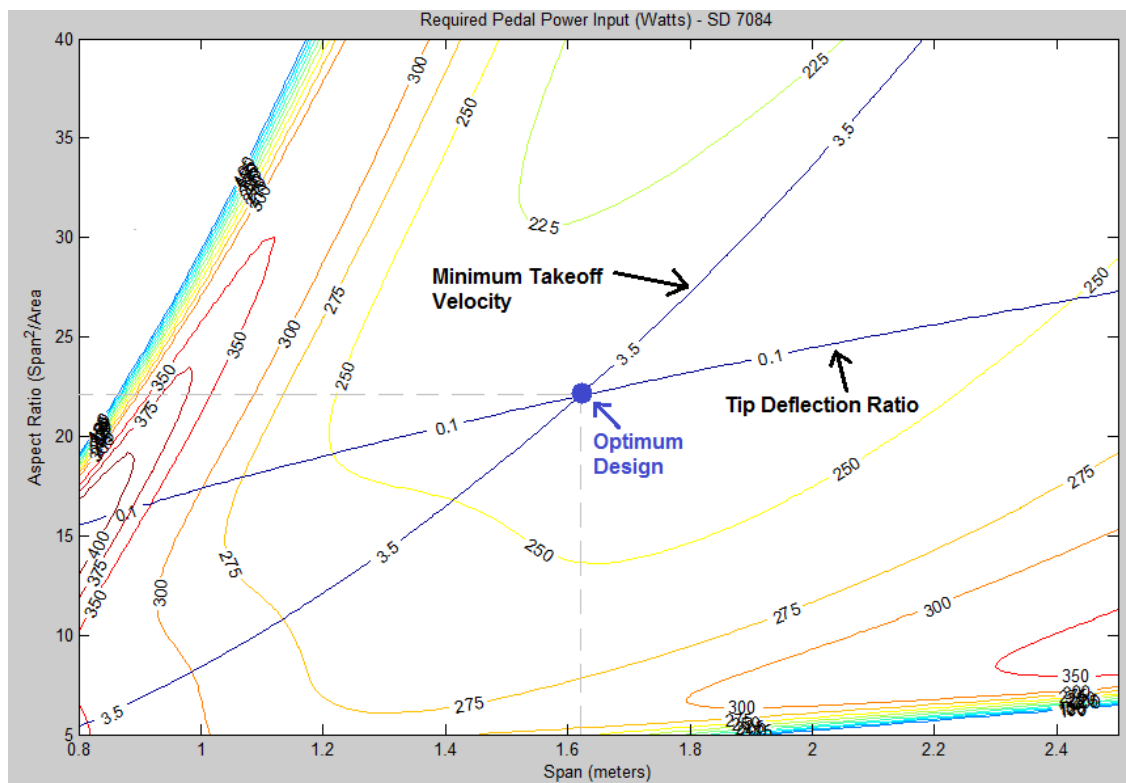


Figure 10. Graphical optimization relating contour plot of required power input, the normalized tip deflection ratio, and maximum takeoff velocity for a SD 7084 foil at design speed. (Normalized tip displacement ratio is the height of tip deflection divided by one half of total wingspan)

The optimization illustrated in Figure 10 indicates that SD 7084 lifting foil with a span of 1.625 meters and an aspect ratio of 22 requires a power input of 240 Watts to cruise at the design velocity of 4.928 m/s. Since a man of average fitness can be expected, according to NASA physiological studies, to sustain a power output of 300 watts for over seven minutes, the vehicle should allow most riders to travel 2000 meters faster than a world record rower.²¹ In light of this data, the human powered hydrofoil with a lifting wing defined by this optimization process is expected to achieve the desired performance goals.

References

- 1 - "The Official World Rowing Web Site - Results/Best Times." *World Rowing - Official Website* //.. Web. 6 Sept. 2010. <<http://www.worldrowing.com/index.php?pageid=87>>
- 2 - Hermanson, M.J., Hudoba, B. "Design of a Second Generation Human-Powered Hydrofoil" *Advances in Bioengineering 20.1 (1991): 551-554*. Print
- 3 - Vellinga, Ray. *Hydrofoils: Design, Build, Fly*. Gig Harbor, WA: Peacock Hill Pub., 2009. Print.
- 4 - "Decavitator History." *Lancet WWW Server*. Web. 23 Sept. 2010. <<http://lancet.mit.edu/decavitator/History.html>>.
- 5, 8,12,13,19,20 - Abbott, Allan V., and David Gordon Wilson. *Human-powered Vehicles*. Champaign, IL: Human Kinetics, 1995. Print. Pgs 80-86
- 6, 10 - Houghton, E. L., and P. W. Carpenter. *Aerodynamics for Engineering Students*. Oxford: Butterworth-Heinemann, 2003. Print.
- 7 - Kuhlman, Bill, and Bunny Kuhlman. "Swept Wings and Effective Dihedral." *RC Soaring Digest* 1 Jan. 2000: 16. Web. 23 Oct. 2010. <<http://www.b2streamlines.com/EffectiveDihedral.pdf>>.
- 11 - Anderson, John David. *Fundamentals of Aerodynamics*. New York: McGraw-Hill, 1991. Print.
- 14 - Munson, Bruce Roy, Donald F. Young, T. H. Okiishi, and Wade W. Huebsch. *Fundamentals of Fluid Mechanics*. Hoboken, NJ: Wiley, 2009. Print. 494,498
- 15 - Katz, Joseph. *Low-speed Aerodynamics*. New York: Cambridge U, 2008. Print. Pg. 7
- 16 - "Airfoil Investigation Database - Search." *Airfoil Investigation Database - Welcome*. Web. Sept.-Oct. 2010. <<http://www.worldofkrauss.com/foils/search>>.
- 17 - Beer, Ferdinand P. *Mechanics of Materials*. New York: McGraw-Hill Higher Education, 2009. Print.
- 18 - *Online Materials Information Resource - MatWeb*. Web. 24 Nov. 2010. <<http://www.matweb.com/>>.
- 20 - Wilson, Dave. "Maximum Human Power" *Human Power* 13.2 (1998): 18-19. Print